HHS Public Access

Author manuscript

Nat Biotechnol. Author manuscript; available in PMC 2015 November 01.

Published in final edited form as:

Nat Biotechnol. 2015 May ; 33(5): 510–517. doi:10.1038/nbt.3199.

Epigenome editing by a CRISPR/Cas9-based acetyltransferase activates genes from promoters and enhancers

Isaac B. Hilton[1,2], **Anthony M. D'Ippolito**[2,3], **Christopher M. Vockley**[2,4], **Pratiksha I. Thakore**[1,2], **Gregory E. Crawford**[2,5], **Timothy E. Reddy**[2,6,*], and **Charles A. Gersbach**[1,2,7,*]

[1]Department of Biomedical Engineering, Duke University, Durham, North Carolina, United States of America

[2]Center for Genomic & Computational Biology, Duke University, Durham, North Carolina, United States of America

[3]University Program in Genetics and Genomics, Duke University Medical Center, Durham, North Carolina, United States of America

[4]Department of Cell Biology, Duke University Medical Center, Durham, North Carolina, United States of America

[5]Department of Pediatrics, Division of Medical Genetics, Duke University Medical Center, Durham, North Carolina, United States of America

[6]Department of Biostatistics & Bioinformatics, Duke University Medical Center, Durham, North Carolina, United States of America

[7]Department of Orthopaedic Surgery, Duke University Medical Center, Durham, North Carolina, United States of America

Abstract

Technologies that facilitate the targeted manipulation of epigenetic marks could be used to precisely control cell phenotype or interrogate the relationship between the epigenome and transcriptional control. Here we have generated a programmable acetyltransferase based on the CRISPR/Cas9 gene regulation system, consisting of the nuclease-null dCas9 protein fused to the catalytic core of the human acetyltransferase p300. This fusion protein catalyzes acetylation of histone H3 lysine 27 at its target sites, corresponding with robust transcriptional activation of

Address for correspondence: Timothy E. Reddy, Ph.D., Center for Genomic & Computational Biology, Box 3382, 101 Science Drive, Duke University, Durham, NC 27708, 919-684-3286, tim.reddy@duke.edu. Charles A. Gersbach, Ph.D., Department of Biomedical Engineering, Room 136 Hudson Hall, Box 90281, Duke University, Durham, NC 27708-0281, 919-613-2147, charles.gersbach@duke.edu.

*Co-corresponding authors

Author Contributions

I.B.H., A.M.D., C.M.V., G.E.C., T.E.R. and C.A.G. designed experiments. I.B.H., A.M.D., and C.M.V. performed the experiments. I.B.H., A.M.D., C.M.V., G.E.C., T.E.R. and C.A.G. analyzed the data. I.B.H. and C.A.G. wrote the manuscript with contributions by all authors.

Conflict of interest statement: C.A.G. and I.B.H. have filed patent applications related to genome engineering technologies. C.A.G. is a scientific advisor to Editas Medicine, a company engaged in therapeutic development of genome engineering technologies.

target genes from promoters, proximal enhancers, and distal enhancers. Gene activation by the targeted acetyltransferase is highly specific across the genome. In contrast to conventional dCas9-based activators, the acetyltransferase effectively activates genes from enhancer regions and with individual guide RNAs. The core p300 domain is also portable to other programmable DNA-binding proteins. These results support targeted acetylation as a causal mechanism of transactivation and provide a new robust tool for manipulating gene regulation.

A primary challenge of functional genomics is to develop technologies that directly and precisely manipulate genome function at individual loci. Projects such as ENCODE[1] and the Roadmap Epigenomics Project[2] have identified millions of epigenetic marks across the human genome for many human cell types and tissues. Studying the function of those marks, however, has been largely limited to statistical associations with gene expression. Technologies for targeted direct manipulation of these epigenetic properties are necessary to transform such association-based findings into mechanistic principles of gene regulation. Such advances have the potential to benefit human health, as they could lead to gene therapies that modify the epigenetic code at targeted regions of the genome, strategies for regenerative medicine and disease modeling based on the epigenetic reprogramming of cell lineage specification, and the engineering of epigenome-specific drug screening platforms.

Manipulation of the epigenome is possible by treating cells with small molecule drugs, such as inhibitors of histone deacetylases or DNA methyltransferases, or differentiating cells into specific lineages. However, small molecule-based methods globally alter the epigenome and transcriptome, and are not suitable for targeting individual loci. Epigenome editing technologies, including the fusion of epigenome-modifying enzymes to programmable DNA-binding proteins such as zinc finger proteins and transcription activator-like effectors (TALEs), have been effective at achieving targeted DNA methylation, DNA hydroxymethylation, and histone demethylation, methylation, and deacetylation[3–8]. However a strategy for targeted histone acetylation, which is strongly associated with active gene regulatory elements and enhancers, has not been described. Additionally, the recent emergence of the CRISPR/Cas9 system as a robust and facile genome engineering platform has the potential to broadly enable epigenome editing across science and technology.

The type II CRISPR/Cas9 system from *Streptococcus pyogenes* (Cas9) is a versatile technology for genome engineering[9, 10]. The Cas9 nuclease can be directed to specific genomic loci via complementarity between an engineered guide RNA (gRNA) and the target site[11–13]. The enzymatic activity of the Cas9 nuclease can be abolished by mutation of the RuvC and HNH domains, generating the nuclease-null deactivated Cas9 (dCas9)[12]. Fused to repression domains, such as the KRAB domain, or activation domains, such as oligomers of the herpes simplex viral protein 16 (VP16), dCas9 can function as a synthetic transcriptional regulator.[14–21] However, limitations in the use of dCas9 activators remain, including the need for multiple activation domains[14, 20, 22, 23] or combinations of gRNAs[16, 17] to achieve high levels of gene induction by synergistic effects between activation domains[24, 25]. The conventional activator domains used in these engineered transcriptional factors, such as the VP16 tetramer VP64[26], function as a scaffold for recruiting multiple components of the preinitiation complex[27, 28] and do not have direct enzymatic function to specifically

modulate the chromatin state. This indirect method of epigenetic remodeling does not allow for testing the role of specific epigenetic marks and may not be as potent as the direct programming of epigenetic states. We hypothesized that recruitment of acetyltransferase function by dCas9 and a gRNA to the genomic target site would directly modulate epigenetic structure, allowing for more effective gene activation. To this end, we rationally designed an effector fusion protein of dCas9 with the catalytic histone acetyltransferase (HAT) core domain of the human E1A-associated protein p300[29]. This is an easily programmable approach that facilitates robust control of the epigenome and downstream gene expression.

Results

A dCas9 fusion to the p300 HAT domain activates target genes

p300 is a highly conserved acetyltransferase involved in a wide range of cellular processes[30, 31]. We fused the full-length p300 protein to dCas9 (dCas9^{FLp300}; Fig. 1a, b) and assayed its capacity for transactivation by transient co-transfection of human HEK293T cells with four gRNAs targeting the endogenous promoters of *IL1RN*, *MYOD1* (*MYOD*), and *POU5F1*/*OCT4 (OCT4)* (Fig. 1c). We used a combination of four gRNAs targeting each promoter based on our and others' previous observations that multiple gRNAs at a single promoter are necessary for robust gene activation[14–22]. dCas9^{FLp300} was well expressed and induced modest activation above background compared to the canonical dCas9 activator fused to the VP64 acidic activation domain (dCas9^{VP64}) (Figs. 1a–c). The full-length p300 protein is a promiscuous acetyltransferase which interacts with a multitude of endogenous proteins, largely via its termini[29, 31]. In order to mitigate these interactions we isolated the contiguous region of full-length p300 (2414 aa) solely required for inherent HAT activity (amino acids 1048-1664), known as the p300 HAT core domain (p300 Core)[29]. When fused to the C-terminus of dCas9 (dCas9$^{p300\ Core}$, Fig. 1a, b) the p300 Core domain induced high levels of transcription from endogenous gRNA-targeted promoters (Fig. 1c). When targeted to the *IL1RN* and *MYOD* promoters, the dCas9$^{p300\ Core}$ fusion displayed significantly higher levels of transactivation than dCas9^{VP64} (*P*-value 0.01924 and 0.0324 respectively; Fig. 1c). These dCas9-effector fusion proteins were expressed at similar levels (Fig. 1b, Supplementary Fig. 1) indicating that the observed differences were due to differences to transactivation capacity. Additionally, no changes to target gene expression were observed when the effector fusions were transfected without gRNAs (Supplementary Fig. 2). To ensure that the p300 Core acetyltransferase activity was responsible for gene transactivation using the dCas9$^{p300\ Core}$ fusion, we screened a panel of dCas9$^{p300\ Core}$ HAT-domain mutant fusion proteins (Supplementary Fig. 1)[29]. A single inactivating amino acid substitution within the HAT core domain (WT residue D1399 of full-length p300) of dCas9$^{p300\ Core}$ (dCas9$^{p300\ Core\ (D1399Y)}$; Fig. 1a) abolished the transactivation capacity of the fusion protein (Fig. 1c), demonstrating that intact p300 Core acetyltransferase activity was required for dCas9$^{p300\ Core}$-mediated transactivation.

dCas9$^{p300\ Core}$ activates genes from proximal and distal enhancers

Although there are many published examples of activating genes with engineered transcription factors targeted to promoters, inducing gene expression from other distal

regulatory elements has been limited, particularly for dCas9-based activators[32–35]. Given the role and localization of p300 at endogenous enhancers[36, 37], we hypothesized that the dCas9$^{p300\ Core}$ would effectively induce transcription from distal regulatory regions with appropriately targeted gRNAs. We targeted the distal regulatory region (DRR) and core enhancer (CE) of the human *MYOD* locus[38] through co-transfection of four gRNAs targeted to each region and either dCas9^{VP64} or dCas9$^{p300\ Core}$ (Fig. 2a). Compared to a mock-transfected control, dCas9^{VP64} did not show any induction when targeted to the *MYOD* DRR or CE region. In contrast, dCas9$^{p300\ Core}$ induced significant transcription when targeted to either *MYOD* regulatory element with corresponding gRNAs (*P*-value 0.0115 and 0.0009 for the CE and DRR regions respectively). We also targeted the upstream proximal (PE) and distal (DE) enhancer regions of the human *OCT4* gene[39] by co-transfection of six gRNAs and either dCas9^{VP64} or dCas9$^{p300\ Core}$ (Fig. 2b). dCas9$^{p300\ Core}$ induced significant transcription from these regions (*P*-value ≤ 0.0001 and *P*-value ≤0.003 for the DE and PE, respectively), whereas dCas9^{VP64} was unable to activate *OCT4* above background levels when targeted to either the PE or DE regions.

The well-characterized mammalian β-globin locus control region (LCR) orchestrates transcription of the downstream hemoglobin genes; hemoglobin epsilon 1 (*HBE*, from ~ 11 kb), hemoglobin gamma 1 and 2 (*HBG*, from ~ 30 kb), hemoglobin delta (*HBD*, from ~ 46 kb), and hemoglobin beta (*HBB*, from ~54 kb) (Fig. 2c)[35, 40]. DNase hypersensitive sites within the β-globin LCR serve as docking sites for transcriptional and chromatin modifiers, including p300[41], which coordinate distal target gene expression. We designed four gRNAs targeting the DNase hypersensitive site 2 within the LCR enhancer region (HS2 enhancer). These four HS2-targeted gRNAs were co-transfected with dCas9, dCas9^{VP64}, dCas9$^{p300\ Core}$, or dCas9$^{p300\ Core\ (D1399Y)}$, and the resulting mRNA production from *HBE*, *HBG*, *HBD*, and *HBB*, was assayed (Fig. 2c). dCas9, dCas9^{VP64}, and dCas9$^{p300\ Core\ (D1399Y)}$ were unable to transactivate any downstream genes when targeted to the HS2 enhancer. In contrast, targeting of dCas9$^{p300\ Core}$ to the HS2 enhancer led to significant expression of the downstream *HBE*, *HBG*, and *HBD* genes (*P*-value ≤ 0.0001, 0.0056, and 0.0003 between dCas9$^{p300\ Core}$ and mock-transfected cells for *HBE*, *HBG*, and *HBD* respectively). Overall, *HBD* and *HBE* appeared relatively less responsive to synthetic p300 Core-mediated activation from the HS2 enhancer; a finding consistent with lower rates of general transcription from these two genes across several cell lines (Supplementary Fig. 3). Nevertheless, with the exception of the most distal *HBB* gene, dCas9$^{p300\ Core}$ exhibited a capacity to activate transcription from downstream genes when targeted to all characterized enhancer regions assayed, a capability not observed for dCas9^{VP64}. Together, these results demonstrate that dCas9$^{p300\ Core}$ is a potent programmable transcription factor that can be used to regulate gene expression from a variety of promoter-proximal and promoter-distal locations.

Gene activation by dCas9$^{p300\ Core}$ is highly specific

Recent reports indicate that dCas9 may have widespread off-target binding events in mammalian cells in combination with some gRNAs[42, 43], which could potentially lead to off-target changes in gene expression. In order to assess the transcriptional specificity of the dCas9$^{p300\ Core}$ fusion protein we performed transcriptome profiling by RNA-seq in cells co-

transfected with four *IL1RN*-targeted gRNAs and either dCas9, dCas9^{VP64}, dCas9$^{p300\ Core}$, or dCas9$^{p300\ Core\ (D1399Y)}$. Genome-wide transcriptional changes were compared between dCas9 with no fused effector domain and either dCas9^{VP64}, dCas9$^{p300\ Core}$, or dCas9$^{p300\ Core\ (D1399Y)}$ (Fig. 3). While both dCas9^{VP64} and dCas9$^{p300\ Core}$ upregulated all four *IL1RN* isoforms, only the effects of dCas9$^{p300\ Core}$ reached genome-wide significance (Fig. 3a–b, Supplementary Table 1; *P*-value 1.0×10^{-3}–5.3×10^{-4} for dCas9^{VP64}; *P*-value 1.8×10^{-17}–1.5×10^{-19} for dCas9$^{p300\ Core}$. In contrast, dCas9$^{p300\ Core\ (D1399Y)}$ did not significantly induce any *IL1RN* expression (Fig. 3c; *P*-value > 0.5 for all 4 *IL1RN* isoforms). Comparative analysis to dCas9 revealed limited dCas9$^{p300\ Core}$ off-target gene induction, with only two transcripts induced significantly above background at a false discovery rate (FDR) < 5%: *KDR* (FDR = 1.4×10^{-3}); and *FAM49A* (FDR = 0.04) (Fig. 3b, Supplementary Table 1). We also found increased expression of *p300* mRNA in cells transfected with dCas9$^{p300\ Core}$ and dCas9$^{p300\ Core\ (D1399Y)}$. This finding is most likely explained by RNA-seq reads mapping to mRNA from the transiently transfected p300 core fusion domains. Thus the dCas9$^{p300\ Core}$ fusion displayed high genome-wide targeted transcriptional specificity and robust gene induction of all four targeted *IL1RN* isoforms.

dCas9$^{p300\ Core}$ acetylates H3K27 at enhancers and promoters

Activity of regulatory elements correlates with covalent histone modifications such as acetylation and methylation[1, 2]. Of those histone modifications, acetylation of lysine 27 on histone H3 (H3K27ac) is one of the most widely documented indicators of enhancer activity[29–31, 36, 37]. Acetylation of H3K27 is catalyzed by p300 and is also correlated with endogenous p300 binding profiles[36, 37]. Therefore we used H3K27ac enrichment as a measurement of relative dCas9$^{p300\ Core}$-mediated acetylation at the genomic target site. To quantify targeted H3K27 acetylation by dCas9$^{p300\ Core}$ we performed chromatin immuno-precipitation with an anti-H3K27ac antibody followed by quantitative PCR (ChIP-qPCR) in HEK293T cells co-transfected with four HS2 enhancer-targeted gRNAs and either dCas9, dCas9^{VP64}, dCas9$^{p300\ Core}$, or dCas9$^{p300\ Core\ (D1399Y)}$ (Fig. 4). We analyzed three amplicons at or around the target site in the HS2 enhancer or within the promoter regions of the *HBE* and *HBG* genes (Fig. 4a). Notably, H3K27ac is enriched in each of these regions in the human K562 erythroid cell line that has a high level of globin gene expression (Fig. 4a). We observed significant H3K27ac enrichment at the HS2 enhancer target locus compared to treatment with dCas9 in both the dCas9^{VP64} (*P*-value 0.0056 for ChIP Region 1and *P*-value 0.0029 for ChIP Region 3) and dCas9$^{p300\ Core}$ (*P*-value 0.0013 for ChIP Region 1and *P*-value 0.0069 for ChIP Region 3) co-transfected samples (Fig. 4b). A similar trend of H3K27ac enrichment was also observed when targeting the *IL1RN* promoter with dCas9^{VP64} or dCas9$^{p300\ Core}$ (Supplementary Fig. 4). In contrast to these increases in H3K27ac at the target sites by both dCas9^{VP64} or dCas9$^{p300\ Core}$, robust enrichment in H3K27ac at the HS2-regulated *HBE* and *HBG* promoters was observed only with dCas9$^{p300\ Core}$ treatment (Fig. 4c–d). Together these results demonstrate that dCas9$^{p300\ Core}$ uniquely catalyzes H3K27ac enrichment at gRNA-targeted loci and at enhancer-targeted distal promoters. Therefore the acetylation established by dCas9$^{p300\ Core}$ at HS2 may catalyze enhancer activity in a manner distinct from direct recruitment of preinitiation complex components by dCas9^{VP64}(refs [27, 28]), as indicated by the distal activation of the

HBE, *HBG*, and *HBD* genes from the HS2 enhancer by dCas9$^{p300\ Core}$ but not by dCas9^{VP64} (Fig. 2c, Supplementary Fig. 3).

dCas9$^{p300\ Core}$ activates genes with a single gRNA

Robust transactivation using dCas9-effector fusion proteins currently relies upon the application of multiple gRNAs, multiple effector domains, or both[14–22, 24, 25]. Transcriptional activation could be simplified with the use of single gRNAs in tandem with a single dCas9-effector fusion. This would also facilitate multiplexing distinct target genes and the incorporation of additional functionalities into the system. We compared the transactivation potential of dCas9$^{p300\ Core}$ with single gRNAs and four pooled gRNAs targeting the *IL1RN*, *MYOD* and *OCT4* promoters (Fig. 5a–c). Substantial activation was observed upon co-transfection of the dCas9$^{p300\ Core}$ and a single gRNA at each promoter tested. For the *IL1RN* and *MYOD* promoters, there was no significant difference between the pooled gRNAs and the best individual gRNA (Fig. 5a–b; *IL1RN* gRNA “C”, *P*-value 0.78; *MYOD* gRNA “D”, *P*-value 0.26). Although activation of the *OCT4* promoter produced additive effects when four gRNAs were pooled with dCas9$^{p300\ Core}$, the most potent single gRNA (gRNA “D”) induced a statistically comparable amount of gene expression to that observed upon co-transfection of dCas9^{VP64} with an equimolar pool of all four promoter gRNAs (*P*-value 0.73; Fig. 5c). Compared to dCas9$^{p300\ Core}$, levels of gene activation with dCas9^{VP64} and single gRNAs were substantially lower. Also, in contrast to dCas9$^{p300\ Core}$, dCas9^{VP64} demonstrated synergistic effects with combinations of gRNAs in every case, (Fig. 5a–c) as reported previously[16, 17].

Based on the transactivation ability of dCas9$^{p300\ Core}$ at enhancer regions and with single gRNAs at promoter regions, we hypothesized that dCas9$^{p300\ Core}$ might also be able to transactivate enhancers via a single targeted gRNA. We tested the *MYOD* (DRR and CE), *OCT4* (PE and DE), and HS2 enhancer regions with equimolar concentrations of pools or single gRNAs (Fig. 5d–g). For both *MYOD* enhancer regions, co-transfection of dCas9$^{p300\ Core}$ and a single enhancer-targeting gRNA was sufficient to activate gene expression to levels similar to cells co-transfected with dCas9$^{p300\ Core}$ and the four pooled enhancer gRNAs (Fig. 5d). Similarly, *OCT4* gene expression was activated from the PE via dCas9$^{p300\ Core}$ localization with a single gRNA to similar levels as dCas9$^{p300\ Core}$ localized with a pool of six PE-targeted gRNAs (Fig. 5e). dCas9$^{p300\ Core}$-mediated induction of *OCT4* from the DE (Fig. 5e) and *HBE* and *HBG* genes from the HS2 enhancer (Fig. 5f–g) showed increased expression with the pooled gRNAs relative to single gRNAs. Nevertheless, there was activation of target gene expression above control for several single gRNAs at these enhancers (Fig. 5e–g).

The p300 HAT domain is portable to other DNA-binding proteins

The dCas9/gRNA system from *Streptococcus pyogenes* has been widely adopted due to its robust, versatile, and easily programmable properties[9, 10]. However, several other programmable DNA-binding proteins are also under development for various applications and may be preferable for particular applications, including orthogonal dCas9 systems from other species[44], TALEs, and zinc finger proteins. To determine if the p300 Core HAT domain was portable to these other systems, we created fusions to dCas9 from *Neisseria*

meningitidis (*Nm*-dCas9)[44], four different TALEs targeting the *IL1RN* promoter[24], and a zinc finger protein targeting *ICAM1* (Fig. 6). Co-transfection of *Nm*-dCas9$^{p300\ Core}$ and five *Nm*-gRNAs targeted to the *HBE* or the *HBG* promoters led to significant gene induction compared to mock-transfected controls (*P*-value 0.038 and 0.0141 for *HBE* and *HBG* respectively) (Fig. 6b–c). When co-transfected with five *Nm*-gRNAs targeted to the HS2 enhancer, *Nm*-dCas9$^{p300\ Core}$ also significantly activated the distal *HBE* and *HBG*, globin genes compared to mock-transfected controls ($p = 0.0192$ and $p=0.0393$, respectively)(Fig. 6d–e). Similar to dCas9$^{p300\ Core}$, *Nm*-dCas9$^{p300\ Core}$ activated gene expression from promoters and the HS2 enhancer via a single gRNA. *Nm*-dCas9^{VP64} displayed negligible capacity to transactivate *HBE* or *HBG* regardless of localization to promoter regions or to the HS2 enhancer either with single or multiple gRNAs (Fig. 6b–e). Transfection of the expression plasmids for a combination of four TALE$^{p300\ Core}$ fusion proteins targeted to the *IL1RN* promoter (*IL1RN* TALE$^{p300\ Core}$) also activated downstream gene expression, although to a lesser extent than four corresponding TALE^{VP64} fusions (*IL1RN* TALE^{VP64}) (Fig. 6f–g). However, single p300 Core effectors were much more potent than single VP64 domains when fused to *IL1RN* TALEs. Interestingly, dCas9$^{p300\ Core}$ directed to any single binding site generated comparable *IL1RN* expression relative to single or pooled *IL1RN* TALE effectors and direct comparisons suggest that dCas9 may be a more robust activator than TALEs when fused to the larger p300 Core fusion domain (Supplementary Figure 5). Finally, the ZF$^{p300\ Core}$ fusion targeted to the *ICAM1* promoter (*ICAM1* ZF$^{p300\ Core}$) also activated its target gene relative to control and at a similar level as ZF^{VP64} (*ICAM1* ZF^{VP64}) (Fig. 6h–i). The versatility of the p300 Core fusion with multiple targeting domains is evidence that this is a robust approach for targeted acetylation and gene regulation. The various p300 core fusion proteins were expressed well, as determined by western blot (Supplementary Fig. 6), but differences in p300 Core activity between different fusion proteins could be attributable to binding affinity or protein folding.

Discussion

These results establish the dCas9$^{p300\ Core}$ fusion protein as a potent and easily programmable tool to synthetically manipulate acetylation at targeted endogenous loci, leading to regulation of proximal and distal enhancer-regulated genes. The intrinsic p300 Core acetyltransferase activity is crucial for this efficacy, as demonstrated by the consistent lack of chromatin modification and transactivation potential of the dCas9$^{p300\ Core\ (D1399Y)}$ acetyltransferase-null mutant (Figs. 1c, 2c, 4b–d, Supplementary Fig. 1). Fusion of the catalytic core domain of p300 to dCas9 resulted in substantially higher transactivation of downstream genes than the direct fusion of full-length p300 protein despite robust protein expression (Fig. 1b, c). This finding may be due to differences in protein structure and function or interactions with other cellular proteins, suggesting that isolation of catalytic core regions is a useful strategy for future programmable epigenome editing tools. The dCas9$^{p300\ Core}$ fusion protein also exhibited an increased transactivation capacity relative to dCas9^{VP64} (Figs. 1c, 2, 3, 5), including in the context of the *Nm*-dCas9 scaffold (Fig. 6b–e). This was especially evident at distal enhancer regions, at which dCas9^{VP64} displayed little, if any, measurable downstream transcriptional activity (Figs. 2, 6d, e), an important finding for applications involving synthetic transcriptional and epigenomic control. Additionally, the

dCas9$^{p300\ Core}$ displayed precise and robust genome-wide transcriptional specificity (Fig. 3, Supplementary Fig. 2).

The observation that targeted acetylation is sufficient for gene activation at an endogenous locus and enhancer is a significant finding of our study. While it is possible that activation or recruitment of other co-factors is involved in the targeted dCas9$^{p300\ Core}$-mediated epigenomic control, only dCas9$^{p300\ Core}$ was capable of potent transcriptional activation and co-enrichment of acetylation at promoters targeted by the epigenetically modified enhancer (Figs. 2c, 3c, d, Supplementary Fig. 3). This distinction is likely the result of differing modes of activity between the two effector domains. While p300 has inherent acetyltransferase activity[29, 30], VP64 relies upon the sequential recruitment of co-factors, including endogenous p300, for HAT activity at sites of transactivation[27, 28]. Hence dCas9^{VP64}-mediated H3K27 acetylation is likely an indirect secondary effect, whereas dCas9$^{p300\ Core}$ likely acetylates target loci directly and in a manner that is dependent upon an intact acetyltransferase domain. Together, these results support a model in which acetylation is a sufficient step in activating enhancer activity at the loci tested here.

The unique activity of dCas9$^{p300\ Core}$ supports its use in elucidating key steps of gene regulation, including dissection of the interplay between the epigenome, regulatory element activity, and gene regulation. For example, the GATA1 transcription factor that is essential for globin gene expression erythroid cells[45] is not expressed in the HEK293T cells used in this study[16]. The observed potent activation of globin gene expression via dCas9$^{p300\ Core}$-mediated acetylation in the absence of GATA1 suggests that the acetylation at the enhancer occurs downstream of GATA1 but upstream of globin gene activation in erythroid cells. Importantly, the greater transactivation potency of primary and direct acetylation by dCas9$^{p300\ Core}$ relative to dCas9^{VP64} suggests that acetylation of additional factors at the target site may also play a substantial role, and this should be a subject of future investigation.

Although synergy has been widely observed with other synthetic transcriptional activators, including dCas9^{VP64} (refs. [8, 15–17, 19–22, 24, 25]), the p300 Core effector domain did not display similar synergy with either additional gRNAs or TALEs (Figs. 5, 6, Supplementary Figs. 3, 5) or in combination with VP64 (Supplementary Fig. 7). Moreover, the p300 Core effector was capable of robustly activating gene expression through a single gRNA at promoters and characterized enhancers (Figs. 5, 6, Supplementary Fig. 3). This effector was also capable of potent gene activation when targeted by a single TALE recognition site (Fig. 6, Supplementary Fig. 5). Interestingly, certain loci appear to be less responsive to transactivation by the localization of a single dCas9$^{p300\ Core}$ effector to a corresponding regulatory region (Fig. 5e–g, Supplementary Fig. 3). This does not appear to be related to chromatin accessibility based on ENCODE data (Supplementary Fig. 8), but may be related to transcription factor occupancy or competition (including endogenous p300; Supplementary Figs. 3, 8), gRNA and genetic composition[46], TSS proximity[14], and/or the underlying local epigenetic circuitry; none of which are mutually exclusive. These factors are relevant to the function of all programmable DNA-binding proteins and would benefit from future efforts to design optimal gRNAs.

Collectively our results demonstrate that the p300 Core acetyltransferase effector domain is a versatile tool for robust and specific targeted transcriptional control. This effector domain is more potent than existing engineered transcription factors made with single activator domains and demonstrates the ability to catalyze specific epigenetic marks with a CRISPR/Cas9-based fusion protein. The results indicate a causal relationship between directed acetylation and subsequent target gene activation. This technology also affords the ability to synthetically transactivate distal genes from putative and known regulatory regions and simplifies transactivation via the application of a single programmable effector and single target site. These capabilities could be significant in enabling genome-wide screens of regulatory element activity and in multiplexing to target several promoters and/or enhancers simultaneously[14, 20, 47]. Furthermore combining dCas9$^{p300\ Core}$ with light-inducible[48] or chemically inducible[49] control will enable the dynamic control of gene activation in space and time. The ability to target the p300 Core domain with orthogonal dCas9s, TALEs, and zinc finger proteins should also facilitate studies of independent targeting of particular effector functions to distinct loci (Fig. 5, Supplementary Fig. 3). This could include multiplexing various activators, repressors, and epigenetic modifiers to precisely control cell phenotype[23, 33, 50] or decipher complex networks of gene regulation. Additionally the mammalian origin of p300 may provide advantages over virally-derived effector domains for *in vivo* applications by minimizing potential immunogenicity.

The synthetic control of transcription and chromatin is a critical component of cellular engineering. Our results suggest that the unique capabilities of dCas9$^{p300\ Core}$ will afford a greater versatility in controlling the epigenetic and transcriptional states of designed biological systems. This system takes advantage of the simple programmability of the CRISPR/Cas9 system to target acetyltransferase activity and complements other recently described epigenetic editing tools, including fusions of demethylases, methyltransferases, and deacetylases[3–7] to generate a more complete set of epigenome editing tools.

Online Methods

Cell lines and transfection

HEK293T cells were procured from the American Tissue Collection Center (ATCC, Manassas VA) through the Duke University Cell Culture Facility. Cells were cultured in Dulbecco's modified Eagle's medium (DMEM) supplemented with 10% FBS and 1% penicillin/streptomycin and maintained at 37°C and 5% CO_2. Transfections were performed in 24-well plates using 375 ng of respective dCas9 expression vector and 125 ng of equimolar pooled or individual gRNA expression vectors mixed with Lipofectamine 2000 (Life Technologies, cat. #11668019) as per manufacturer's instruction. For ChIP-qPCR experiments, HEK293T cells were transfected in 15 cm dishes with Lipofectamine 2000 and 30 μg of respective dCas9 expression vector and 10 μg of equimolar pooled gRNA expression vectors as per manufacturer's instruction.

Plasmid constructs

pcDNA-dCas9^{VP64} (dCas9^{VP64}; Addgene, plasmid #47107) has been described previously[16]. An HA epitope tag was added to dCas9 (no effector) by removing the VP64

effector domain from dCas9^{VP64} via AscI/PacI restriction sites and using isothermal assembly[51] to include an annealed set of oligos containing the appropriate sequence as per manufacturers instruction (NEB cat. #2611). pcDNA-dCas9^{FLp300} (dCas9^{FLp300}) was created by amplifying full-length p300 from pcDNA3.1-p300 (Addgene, plasmid #23252)[52] in two separate fragments and cloning these fragments into the dCas9^{VP64} backbone via isothermal assembly. A substitution in the full-length p300 protein (L553M), located outside of the HAT Core region, was identified in dCas9^{FLp300} and in the precursor pcDNA3.1-p300 during sequence validation. pcDNA-dCas9$^{p300\ Core}$ (dCas9$^{p300\ Core}$) was generated by first amplifying amino acids 1048 – 1664 of human p300 from cDNA and then subcloning the resulting amplicon into pCR-Blunt (pCR-Blunt$^{p300\ Core}$) (Life Technologies cat. #K2700). An AscI site, HA-epitope tag, and a PmeI site were added by PCR amplification of the p300 Core from pCR-Blunt$^{p300\ Core}$ and subsequently this amplicon was cloned into pCR-Blunt (pCR-Blunt$^{p300\ Core\ +\ HA}$) (Life Technologies cat. #K2700). The HA-tagged p300 Core was cloned from pCR-Blunt$^{p300\ Core\ +\ HA}$ into the dCas9^{VP64} backbone via shared AscI/PmeI restriction sites. pcDNA-dCas9$^{p300\ Core\ (D1399Y)}$ (dCas9$^{p300\ Core\ (D1399Y)}$) was generated by amplification of the p300 Core from dCas9$^{p300\ Core}$ in overlapping fragments with primer sets including the specified nucleic acid mutations, with a subsequent round of linkage PCR and cloning into the dCas9$^{p300\ Core}$ backbone using shared AscI/PmeI restriction sites. All PCR amplifications were carried out using Q5 high-fidelity DNA polymerase (NEB cat. #M0491). Protein sequences of all dCas9 constructs are shown in Supplementary Note 1.

IL1RN, *MYOD*, and *OCT4* promoter gRNA protospacers have been described previously[16, 53]. *Neisseria meningitidis* dCas9^{VP64} (*Nm*-dCas9^{VP64}) was obtained from Addgene (plasmid #48676)[44]. *Nm*-dCas9$^{p300\ Core}$ was created by amplifying the HA-tagged p300 Core from dCas9$^{p300\ Core}$ with primers to facilitate subcloning into the AleI/AgeI-digested *Nm*-dCas9^{VP64} backbone using isothermal assembly (NEB cat. # 2611). *IL1RN* TALE$^{p300\ Core}$ TALEs were generated by subcloning the HA-tagged p300 Core domain from dCas9$^{p300\ Core}$ into previously published[24] *IL1RN* TALE^{VP64} constructs via shared AscI/PmeI restriction sites. *IL1RN* TALE target sites are shown in Supplementary Table 2. *ICAM1* ZF^{VP64} and *ICAM1* ZF$^{p300\ Core}$ were constructed by subcloning the *ICAM1* ZF from pMX-CD54-31Opt-VP64[54] into dCas9^{VP64} and dCas9$^{p300\ Core}$ backbones, respectively, using isothermal assembly (NEB cat. #2611). Protein sequences of *ICAM1* ZF constructs are shown in Supplementary Note 2. Transfection efficiency was routinely above 90% as assayed by co-transfection of PL-SIN-EF1α-EGFP (Addgene plasmid #21320)[55] and gRNA empty vector in all experiments. All *Streptococcus pyogenes* gRNAs were annealed and cloned into pZdonor-pSPgRNA (Addgene plasmid # 47108)[16] for expression as described previously[13] with slight modifications using NEB BbsI and T4 ligase (Cat. #s R0539 and M0202). *Nm*-dCas9 gRNA oligos were rationally designed using published PAM requirements[44], and then cloned into pZDonor-Nm-Cas9-gRNA-hU6 (Addgene, plasmid #61366) via BbsI sites. Plasmids are available through Addgene (Supplementary Table 3). All gRNA protospacer targets are listed in Supplementary Table 4.

Western Blotting

20 μg of protein was loaded for SDS PAGE and transferred onto a nitrocellulose membrane for western blots. Primary antibodies (α-FLAG; Sigma-Aldrich cat. #F7425 and α-GAPDH; Cell Signaling Technology cat. #14C10) were used at a 1:1000 dilution in TBST + 5% Milk. Secondary α-Rabbit HRP (Sigma-Aldrich cat. #A6154) was used at a 1:5000 dilution in TBST + 5% Milk. Membranes were exposed after addition of ECL (Bio-Rad cat. #170-5060).

Quantitative reverse-transcription PCR

RNA was isolated from transfected cells using the RNeasy Plus mini kit (Qiagen cat. #74136) and 500 ng of purified RNA was used as template for cDNA synthesis (Life Technologies, cat. #11754). Real-time PCR was performed using PerfeCTa SYBR Green FastMix (Quanta Biosciences, cat. #95072) and a CFX96 Real-Time PCR Detection System with a C1000 Thermal Cycler (Bio-Rad). Baselines were subtracted using the baseline subtraction curve fit analysis mode and thresholds were automatically calculated using the Bio-Rad CFX Manager software version 2.1. Results are expressed as fold change above control mock transfected cells (No DNA) after normalization to GAPDH expression using the ΔΔCt method as previously described[56]. All qPCR primers and conditions are listed in Supplementary Table 5.

RNA-seq

RNA-seq was performed using three replicates per experimental condition. RNA was isolated from transfected cells using the RNeasy Plus mini kit (Qiagen cat. #74136) and 1 μg of purified mRNA was used as template for cDNA synthesis and library construction using the PrepX RNA-Seq Library Kit (Wafergen Biosystems, cat. #400039). Libraries were prepared using the Apollo 324 liquid handling platform, as per manufacturer's instruction. Indexed libraries were validated for quality and size distribution using the Tapestation 2200 (Agilent) and quantified by qPCR using the KAPA Library Quantification Kit (KAPA Biosystems; KK4835) prior to multiplex pooling and sequencing at the Duke University Genome Sequencing Shared Resource facility. Libraries were pooled and then 50 bp single-end reads were sequenced on a Hiseq 2500 (Illumina), de-multiplexed and then aligned to the HG19 transcriptome using Bowtie 2[57]. Transcript abundance was calculated using the SAMtools[58] suite and differential expression was determined in R using the DESeq2 analysis package. Multiple hypothesis correction was performed using the method of Benjamini and Hochberg with a FDR of < 5%. RNA-seq data is deposited in the NCBI's Gene Expression Omnibus and is accessible through GEO Series accession number GSE66742.

ChIP-qPCR

HEK293T cells were co-transfected with four HS2 enhancer gRNA constructs and indicated dCas9 fusion expression vectors in 15 cm plates in biological triplicate for each condition tested. Cells were cross-linked with 1% Formaldehyde (final concentration; Sigma F8775-25ML) for 10 min at RT and then the reaction was stopped by the addition of glycine to a final concentration of 125 mM. From each plate ~2.5e7 cells were used for H3K27ac

ChIP-enrichment. Chromatin was sheared to a median fragment size of 250 bp using a Bioruptor XL (Diagenode). H3K27ac enrichment was performed by incubation with 5 μg of Abcam ab4729 and 200 μl of sheep anti-rabbit IgG magnetic beads (Life Technologies 11203D) for 16 hrs at 4°. Cross-links were reversed via overnight incubation at 65°C with sodium dodecyl sulfate, and DNA was purified using MinElute DNA purification columns (Qiagen). 10ng of DNA was used for subsequent qPCR reactions using a CFX96 Real-Time PCR Detection System with a C1000 Thermal Cycler (Bio-Rad). Baselines were subtracted using the baseline subtraction curve fit analysis mode and thresholds were automatically calculated using the Bio-Rad CFX Manager software version 2.1. Results are expressed as fold change above cells co-transfected with dCas9 and four HS2 gRNAs after normalization to β-actin enrichment using the ΔΔCt method as previously described[56]. All ChIP-qPCR primers and conditions are listed in Supplementary Table 5.

Supplementary Material

Refer to Web version on PubMed Central for supplementary material.

Acknowledgments

Pablo Perez-Pinera, Pratiksha Thakore, Dewran Kocak, David Ousterout, and Darrin Lim provided assistance with gRNA design, plasmid cloning, PCR primer validation, and/or RNA isolations. The gene encoding the *ICAM1*-targeted zinc finger protein was provided by Carlos Barbas, III. This work was supported by a US National Institutes of Health (NIH) grants to G.E.C., C.A.G., and T.E.R. (R01DA036865 and U01HG007900), a NIH Director's New Innovator Award (DP2OD008586) and National Science Foundation (NSF) Faculty Early Career Development (CAREER) Award (CBET-1151035) to C.A.G., and NIH grant P30AR066527.

References

1. Dunham I, et al. An integrated encyclopedia of DNA elements in the human genome. Nature. 2012; 489:57–74. [PubMed: 22955616]
2. Bernstein BE, et al. The NIH Roadmap Epigenomics Mapping Consortium. Nat Biotechnol. 2010; 28:1045–1048. [PubMed: 20944595]
3. Snowden AW, Gregory PD, Case CC, Pabo CO. Gene-specific targeting of H3K9 methylation is sufficient for initiating repression in vivo. Curr Biol. 2002; 12:2159–2166. [PubMed: 12498693]
4. Maeder ML, et al. Targeted DNA demethylation and activation of endogenous genes using programmable TALE-TET1 fusion proteins. Nat Biotechnol. 2013; 31:1137–1142. [PubMed: 24108092]
5. Mendenhall EM, et al. Locus-specific editing of histone modifications at endogenous enhancers. Nat Biotechnol. 2013; 31:1133–1136. [PubMed: 24013198]
6. Rivenbark AG, et al. Epigenetic reprogramming of cancer cells via targeted DNA methylation. Epigenetics. 2012; 7:350–360. [PubMed: 22419067]
7. Konermann S, et al. Optical control of mammalian endogenous transcription and epigenetic states. Nature. 2013; 500:472–476. [PubMed: 23877069]
8. Keung AJ, Bashor CJ, Kiriakov S, Collins JJ, Khalil AS. Using targeted chromatin regulators to engineer combinatorial and spatial transcriptional regulation. Cell. 2014; 158:110–120. [PubMed: 24995982]
9. Hsu PD, Lander ES, Zhang F. Development and applications of CRISPR-Cas9 for genome engineering. Cell. 2014; 157:1262–1278. [PubMed: 24906146]
10. Doudna JA, Charpentier E. Genome editing. The new frontier of genome engineering with CRISPR-Cas9. Science. 2014; 346:1258096. [PubMed: 25430774]
11. Mali P, et al. RNA-guided human genome engineering via Cas9. Science. 2013; 339:823–826. [PubMed: 23287722]

12. Jinek M, et al. A programmable dual-RNA-guided DNA endonuclease in adaptive bacterial immunity. Science. 2012; 337:816–821. [PubMed: 22745249]
13. Cong L, et al. Multiplex genome engineering using CRISPR/Cas systems. Science. 2013; 339:819–823. [PubMed: 23287718]
14. Konermann S, et al. Genome-scale transcriptional activation by an engineered CRISPR-Cas9 complex. Nature. 2015; 517:583–588. [PubMed: 25494202]
15. Mali P, et al. CAS9 transcriptional activators for target specificity screening and paired nickases for cooperative genome engineering. Nat Biotechnol. 2013; 31:833–838. [PubMed: 23907171]
16. Perez-Pinera P, et al. RNA-guided gene activation by CRISPR-Cas9-based transcription factors. Nature methods. 2013; 10:973–976. [PubMed: 23892895]
17. Maeder ML, et al. CRISPR RNA-guided activation of endogenous human genes. Nat Methods. 2013; 10:977–979. [PubMed: 23892898]
18. Qi LS, et al. Repurposing CRISPR as an RNA-guided platform for sequence-specific control of gene expression. Cell. 2013; 152:1173–1183. [PubMed: 23452860]
19. Gilbert LA, et al. CRISPR-mediated modular RNA-guided regulation of transcription in eukaryotes. Cell. 2013; 154:442–451. [PubMed: 23849981]
20. Cheng AW, et al. Multiplexed activation of endogenous genes by CRISPR-on, an RNA-guided transcriptional activator system. Cell Res. 2013; 23:1163–1171. [PubMed: 23979020]
21. Farzadfard F, Perli SD, Lu TK. Tunable and multifunctional eukaryotic transcription factors based on CRISPR/Cas. ACS synthetic biology. 2013; 2:604–613. [PubMed: 23977949]
22. Tanenbaum ME, Gilbert LA, Qi LS, Weissman JS, Vale RD. A protein-tagging system for signal amplification in gene expression and fluorescence imaging. Cell. 2014; 159:635–646. [PubMed: 25307933]
23. Chavez A, et al. Highly efficient Cas9-mediated transcriptional programming. Nature methods. 2015
24. Perez-Pinera P, et al. Synergistic and tunable human gene activation by combinations of synthetic transcription factors. Nat Methods. 2013; 10:239–242. [PubMed: 23377379]
25. Maeder ML, et al. Robust, synergistic regulation of human gene expression using TALE activators. Nat Methods. 2013; 10:243–245. [PubMed: 23396285]
26. Beerli RR, Dreier B, Barbas CF 3rd. Positive and negative regulation of endogenous genes by designed transcription factors. Proc Natl Acad Sci U S A. 2000; 97:1495–1500. [PubMed: 10660690]
27. Choy B, Green MR. Eukaryotic activators function during multiple steps of preinitiation complex assembly. Nature. 1993; 366:531–536. [PubMed: 8255291]
28. Memedula S, Belmont AS. Sequential recruitment of HAT and SWI/SNF components to condensed chromatin by VP16. Current biology: CB. 2003; 13:241–246. [PubMed: 12573221]
29. Delvecchio M, Gaucher J, Aguilar-Gurrieri C, Ortega E, Panne D. Structure of the p300 catalytic core and implications for chromatin targeting and HAT regulation. Nature structural & molecular biology. 2013; 20:1040–1046.
30. Ogryzko VV, Schiltz RL, Russanova V, Howard BH, Nakatani Y. The transcriptional coactivators p300 and CBP are histone acetyltransferases. Cell. 1996; 87:953–959. [PubMed: 8945521]
31. Chen J, Li Q. Life and death of transcriptional co-activator p300. Epigenetics: official journal of the DNA Methylation Society. 2011; 6:957–961.
32. Gao X, et al. Comparison of TALE designer transcription factors and the CRISPR/dCas9 in regulation of gene expression by targeting enhancers. Nucleic Acids Res. 2014; 42:e155. [PubMed: 25223790]
33. Gao X, et al. Reprogramming to Pluripotency Using Designer TALE Transcription Factors Targeting Enhancers. Stem cell reports. 2013; 1:183–197. [PubMed: 24052952]
34. Ji Q, et al. Engineered zinc-finger transcription factors activate OCT4 (POU5F1), SOX2, KLF4, c-MYC (MYC) and miR302/367. Nucleic acids research. 2014; 42:6158–6167. [PubMed: 24792165]
35. Deng W, et al. Reactivation of developmentally silenced globin genes by forced chromatin looping. Cell. 2014; 158:849–860. [PubMed: 25126789]

36. Rada-Iglesias A, et al. A unique chromatin signature uncovers early developmental enhancers in humans. Nature. 2011; 470:279–283. [PubMed: 21160473]
37. Visel A, et al. ChIP-seq accurately predicts tissue-specific activity of enhancers. Nature. 2009; 457:854–858. [PubMed: 19212405]
38. Chen JC, Love CM, Goldhamer DJ. Two upstream enhancers collaborate to regulate the spatial patterning and timing of MyoD transcription during mouse development. Dev Dyn. 2001; 221:274–288. [PubMed: 11458388]
39. Nordhoff V, et al. Comparative analysis of human, bovine, and murine Oct-4 upstream promoter sequences. Mammalian genome: official journal of the International Mammalian Genome Society. 2001; 12:309–317. [PubMed: 11309664]
40. Carter D, Chakalova L, Osborne CS, Dai YF, Fraser P. Long-range chromatin regulatory interactions in vivo. Nature genetics. 2002; 32:623–626. [PubMed: 12426570]
41. Kim YW, Kim A. Histone acetylation contributes to chromatin looping between the locus control region and globin gene by influencing hypersensitive site formation. Biochimica et biophysica acta. 2013; 1829:963–969. [PubMed: 23607989]
42. Kuscu C, Arslan S, Singh R, Thorpe J, Adli M. Genome-wide analysis reveals characteristics of off-target sites bound by the Cas9 endonuclease. Nature biotechnology. 2014; 32:677–683.
43. Wu X, et al. Genome-wide binding of the CRISPR endonuclease Cas9 in mammalian cells. Nature biotechnology. 2014; 32:670–676.
44. Esvelt KM, et al. Orthogonal Cas9 proteins for RNA-guided gene regulation and editing. Nat Methods. 2013; 10:1116–1121. [PubMed: 24076762]
45. Su MY, et al. Identification of biologically relevant enhancers in human erythroid cells. The Journal of biological chemistry. 2013; 288:8433–8444. [PubMed: 23341446]
46. Doench JG, et al. Rational design of highly active sgRNAs for CRISPR-Cas9-mediated gene inactivation. Nature biotechnology. 2014; 32:1262–1267.
47. Gilbert LA, et al. Genome-Scale CRISPR-Mediated Control of Gene Repression and Activation. Cell. 2014; 159:647–661. [PubMed: 25307932]
48. Polstein LR, Gersbach CA. A light-inducible CRISPR-Cas9 system for control of endogenous gene activation. Nature chemical biology. 2015; 11:198–200. [PubMed: 25664691]
49. Zetsche B, Volz SE, Zhang F. A split-Cas9 architecture for inducible genome editing and transcription modulation. Nature biotechnology. 2015; 33:139–142.
50. Chakraborty S, et al. A CRISPR/Cas9-Based System for Reprogramming Cell Lineage Specification. Stem cell reports. 2014; 3:940–947. [PubMed: 25448066]
51. Gibson DG, et al. Enzymatic assembly of DNA molecules up to several hundred kilobases. Nature methods. 2009; 6:343–345. [PubMed: 19363495]
52. Chen LF, Mu Y, Greene WC. Acetylation of RelA at discrete sites regulates distinct nuclear functions of NF-kappaB. The EMBO journal. 2002; 21:6539–6548. [PubMed: 12456660]
53. Hu J, et al. Direct activation of human and mouse Oct4 genes using engineered TALE and Cas9 transcription factors. Nucleic Acids Res. 2014; 42:4375–4390. [PubMed: 24500196]
54. Magnenat L, Blancafort P, Barbas CF 3rd. In vivo selection of combinatorial libraries and designed affinity maturation of polydactyl zinc finger transcription factors for ICAM-1 provides new insights into gene regulation. Journal of molecular biology. 2004; 341:635–649. [PubMed: 15288776]
55. Hotta A, et al. Isolation of human iPS cells using EOS lentiviral vectors to select for pluripotency. Nature methods. 2009; 6:370–376. [PubMed: 19404254]
56. Schmittgen TD, Livak KJ. Analyzing real-time PCR data by the comparative C(T) method. Nature protocols. 2008; 3:1101–1108. [PubMed: 18546601]
57. Langmead B, Salzberg SL. Fast gapped-read alignment with Bowtie 2. Nature methods. 2012; 9:357–359. [PubMed: 22388286]
58. Li H, et al. The Sequence Alignment/Map format and SAMtools. Bioinformatics. 2009; 25:2078–2079. [PubMed: 19505943]

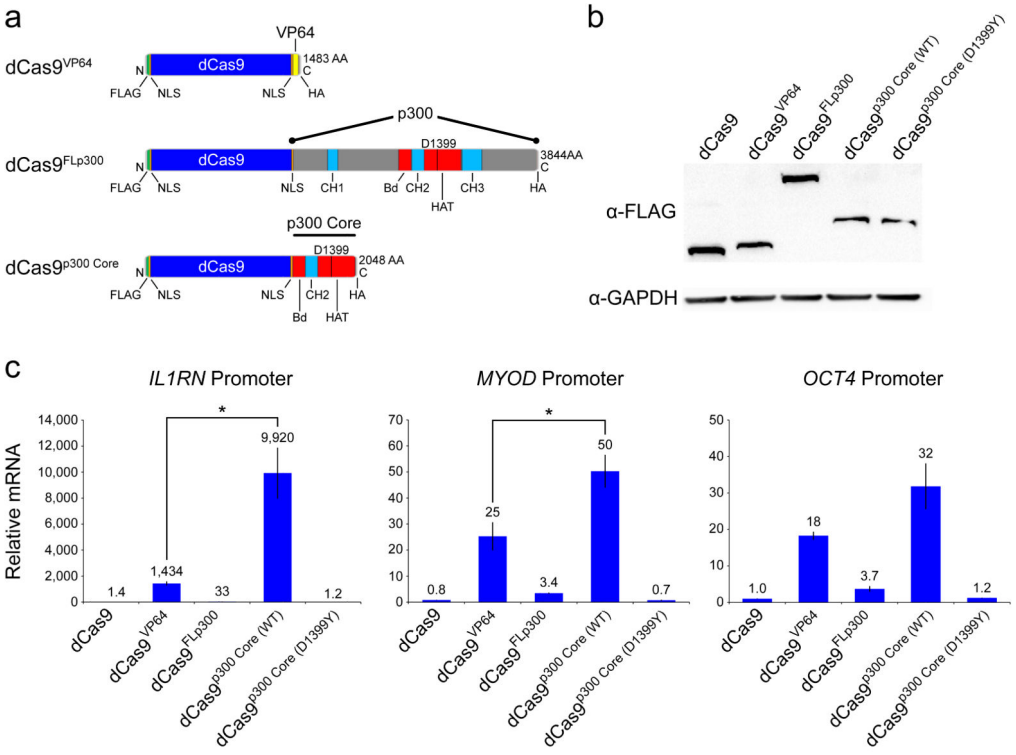

Figure 1.

The dCas9$^{p300\ Core}$ fusion protein activates transcription of endogenous genes from proximal promoter regions. (**a**) Schematic of dCas9 fusion proteins dCas9^{VP64}, dCas9$^{FL\ p300}$, and dCas9$^{p300\ Core}$. *Streptococcus pyogenes* dCas9 contains nuclease inactivating mutations D10A and H840A. The D1399 catalytic residue in the p300 HAT domain is indicated. (**b**) Western blot showing expression levels of dCas9 fusion proteins and GAPDH in co-transfected cells (full blot shown in Supplementary Fig. 1c). (**c**) Relative mRNA expression of *IL1RN*, *MYOD*, and *OCT4*, determined by qRT-PCR, by the indicated dCas9 fusion protein co-transfected with four gRNAs targeted to each promoter region (Tukey-test, **P*-value < 0.05, n = 3 independent experiments each, error bars: s.e.m.). Numbers above bars indicate mean expression. FLAG, epitope tag; NLS, nuclear localization signal; HA, hemagglutinin epitope tag; CH, cysteine-histidine-rich region; Bd, bromodomain; HAT, histone acetyltransferase domain.

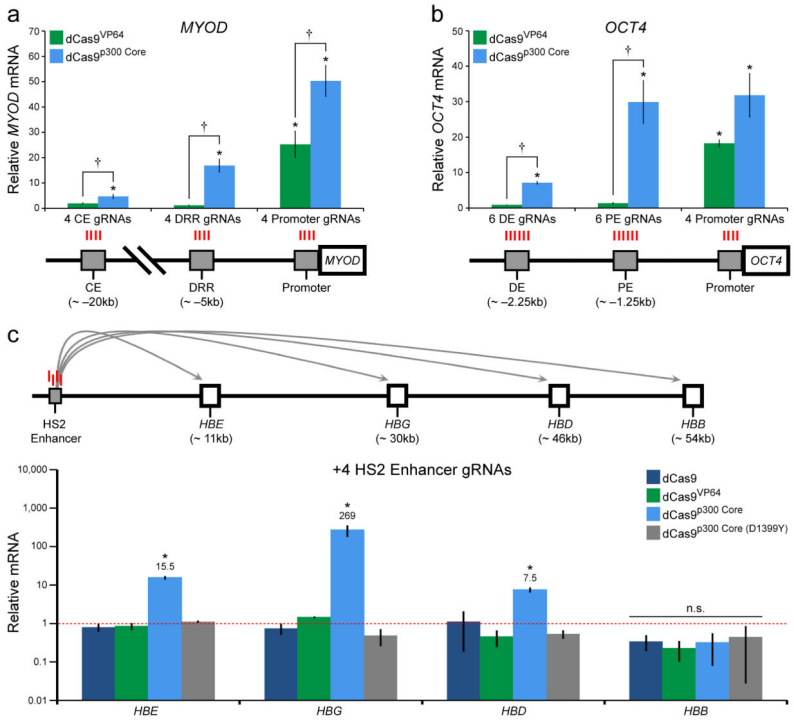

Figure 2.

The dCas9$^{p300\ Core}$ fusion protein activates transcription of endogenous genes from distal enhancer regions. (**a**) Relative *MYOD* mRNA production in cells co-transfected with a pool of gRNA**s** targeted to either the proximal or distal regulatory regions and dCas9^{VP64} or dCas9$^{p300\ Core}$; promoter data from Fig. 1c (Tukey-test, **P*-value <0.05 compared to mock-transfected cells, Tukey test †*P*-value <0.05 between dCas9$^{p300\ Core}$ and dCas9^{VP64}, n = 3 independent experiments, error bars: s.e.m.). The human *MYOD* locus is schematically depicted with corresponding gRNA locations in red. CE, MyoD core enhancer; DRR, MyoD distal regulatory region. (**b**) Relative *OCT4* mRNA production in cells co-transfected with a pool of gRNAs targeted to the proximal and distal regulatory regions and dCas9^{VP64} or dCas9$^{p300\ Core}$; promoter data from Fig. 1c (Tukey-test, **P*-value <0.05 compared to mock-transfected cells, Tukey test †*P*-value <0.05 between dCas9$^{p300\ Core}$ and dCas9^{VP64}, n = 3 independent experiments, error bars: s.e.m.). The human *OCT4* locus is schematically depicted with corresponding gRNA locations in red. DE, Oct4 distal enhancer; PE, Oct4 proximal enhancer. (**c**) The human β-globin locus is schematically depicted with approximate locations of the hypersensitive site 2 (HS2) enhancer region and downstream genes (*HBE*, *HBG*, *HBD*, and *HBB*). Corresponding HS2 gRNA locations are shown in red. Relative mRNA production from distal genes in cells co-transfected with four gRNAs targeted to the HS2 enhancer and the indicated dCas9 proteins. Note logarithmic y-axis and dashed red line indicating background expression (Tukey test among conditions for each β-globin gene, †*P*-value <0.05, n = 3 independent experiments, error bars: s.e.m.). n.s., not significant.

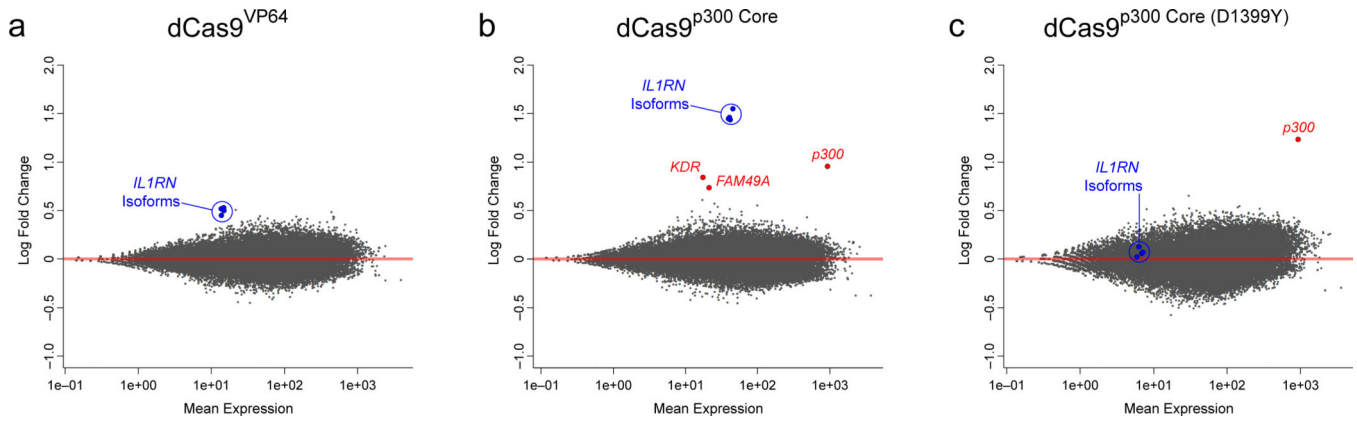

Figure 3.

dCas9$^{p300\ Core}$ targeted transcriptional activation is specific and robust. (**a–c**) MA plots generated from DEseq2 analysis of genome-wide RNA-seq data from HEK293T cells transiently co-transfected with dCas9^{VP64} (**a**) dCas9$^{p300\ Core}$ (**b**) or dCas9$^{p300\ Core\ (D1399Y)}$ (**c**) and four *IL1RN* promoter-targeting gRNAs compared to HEK293T cells transiently co-transfected with dCas9 and four *IL1RN* promoter-targeting gRNAs. mRNAs corresponding to *IL1RN* isoforms are shown in blue and circled in each panel. Red labeled points in panels b–c correspond to off-target transcripts significantly enriched after multiple hypothesis testing (*KDR*, (FDR = 1.4×10^{-3}); *FAM49A*, (FDR = 0.04); *p300*, (FDR = 1.7×10^{-4}) in panel **b**; and *p300*, (FDR = 4.4×10^{-10}) in panel **c**.

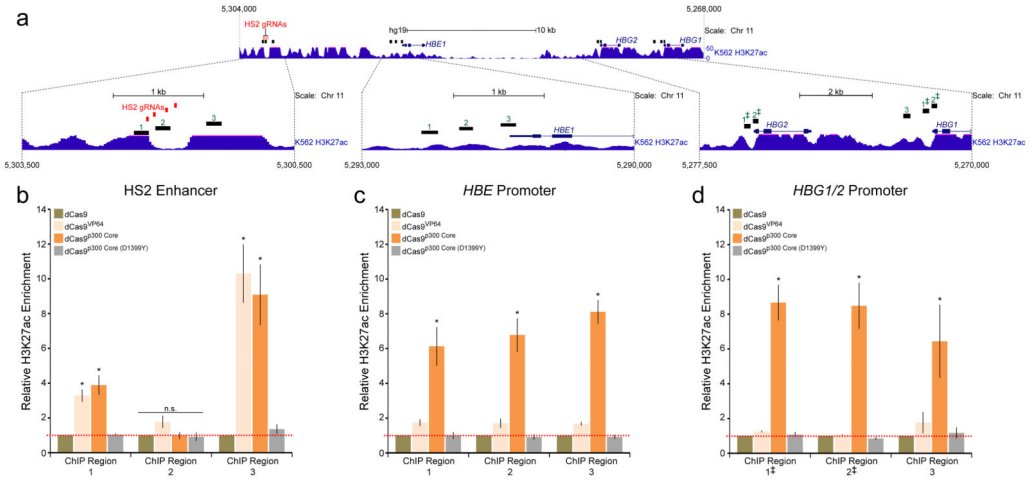

Figure 4.

The dCas9$^{p300\ Core}$ fusion protein acetylates chromatin at a targeted enhancer and corresponding downstream genes. (**a**) The region encompassing the human β-globin locus on chromosome 11 (5,304,000 – 5,268,000; GRCh37/hg19 assembly) is shown. HS2 gRNA target locations are indicated in red and ChIP-qPCR amplicon regions are depicted in black with corresponding green numbers. ENCODE/Broad Institute H3K27ac enrichment signal in K562 cells is shown for comparison. Magnified insets for the HS2 enhancer, *HBE*, and *HBG1/2* promoter regions are displayed below. (**b–d**) H3K27ac ChIP-qPCR enrichment (relative to dCas9; red dotted line) at the HS2 enhancer, *HBE* promoter, and *HBG1/2* promoters in cells co-transfected with four gRNAs targeted to the HS2 enhancer and the indicated dCas9 fusion protein. *HBG* ChIP amplicons 1 and 2 amplify redundant sequences at the *HBG1* and *HBG2* promoters (denoted by ‡). Tukey test among conditions for each ChIP-qPCR region, **P*-value <0.05 (n = 3 independent experiments, error bars: s.e.m.).

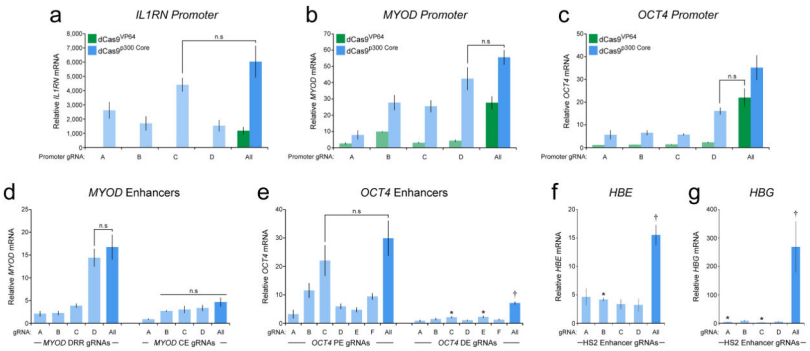

Figure 5.

The dCas9$^{p300\ Core}$ fusion protein activates transcription of endogenous genes from regulatory regions with a single gRNA. (**a–c**) Relative (**a**) *IL1RN*, (**b**) *MYOD* or (**c**) *OCT4* mRNA produced from cells co-transfected with dCas9$^{p300\ Core}$ or dCas9^{VP64} and gRNAs targeting respective promtoters (n = 3 independent experiments, error bars: s.e.m.). Relative *MYOD* (**d**) or *OCT4* (**e**) mRNA produced from cells co-transfected with dCas9$^{p300\ Core}$ and indicated gRNAs targeting the indicated *MYOD or OCT4* enhancers (n = 3 independent experiments, error bars: s.e.m.). DRR, *MYOD* distal regulatory region; CE, *MYOD* core enhancer; PE, *OCT4* proximal enhancer; DE, *OCT4* distal enhancer. (Tukey test between dCas9$^{p300\ Core}$ and single *OCT4* DE gRNAs compared to mock-transfected cells, **P*-value <0.05, Tukey test among dCas9$^{p300\ Core}$ and *OCT4* DE gRNAs compared to All, †*P*-value <0.05,). Relative *HBE* (**f**) or *HBG* (**g**) mRNA production in cells co-transfected with dCas9$^{p300\ Core}$ and the indicated gRNAs targeted to the HS2 enhancer (Tukey test between dCas9$^{p300\ Core}$ and single HS2 gRNAs compared to mock-transfected cells, **P*-value <0.05, Tukey test among dCas9$^{p300\ Core}$ and HS2 single gRNAs compared to All, †*P*<0.05, n = 3 independent experiments, error bars: s.e.m.). HS2, β-globin locus control region hypersensitive site 2; n.s., not significant using Tukey test.

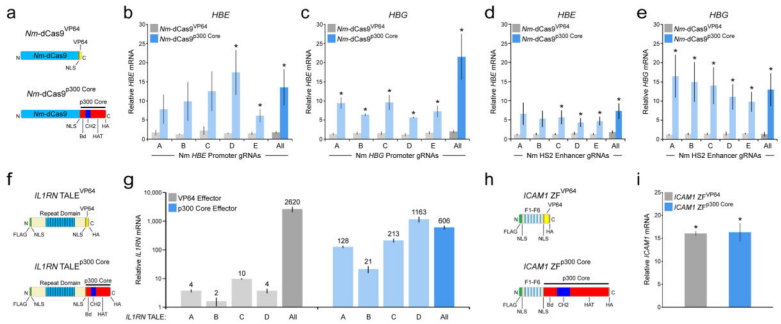

Figure 6.

The p300 Core can be targeted to genomic loci by diverse programmable DNA-binding proteins. (**a**) Schematic of the *Neisseria meningitidis (Nm)* dCas9 fusion proteins *Nm*-dCas9^{VP64} and *Nm*-dCas9$^{p300\ Core}$. *Neisseria meningitidis* dCas9 contains nuclease-inactivating mutations D16A, D587A, H588A, and N611A. (**b–c**) Relative (**b**) *HBE* or (**c**) *HBG* mRNA in cells co-transfected with five individual or pooled (A–E) *Nm* gRNAs targeted to the *HBE* or *HBG* promoter and *Nm*-dCas9^{VP64} or *Nm*-dCas9$^{p300\ Core}$. (**d–e**) Relative (**d**) *HBE* or (**e**) *HBG* mRNA in cells co-transfected with five individual or pooled (A–E) *Nm* gRNAs targeted to the HS2 enhancer and *Nm*-dCas9^{VP64} or *Nm*-dCas9$^{p300\ Core}$. (**f**) Schematic of TALEs with domains containing *IL1RN*-targeted repeat variable diresidues (Repeat Domain). (**g**) Relative *IL1RN* mRNA in cells transfected with individual or pooled (A–D) *IL1RN* TALE^{VP64} or *IL1RN* TALE$^{p300\ Core}$ encoding plasmids. (**h**) Schematic of ZF fusion proteins with zinc finger helices 1–6 (F1–F6) targeting the *ICAM1* promoter. (**i**) Relative *ICAM1* mRNA in cells transfected with *ICAM1* ZF^{VP64} or *ICAM1* ZF$^{p300\ Core}$. Tukey-test, **P*-value <0.05 compared to mock-transfected control, n = 3 independent experiments each, error bars: s.e.m. NLS, nuclear localization signal; HA, hemagglutinin tag; Bd, bromodomain; CH, cysteine-histidine-rich region; HAT, histone acetyltransferase domain.